AD-776 297

APPLICATION OF PRACTICAL OPTIMAL CONTROL THEORY TO THE C-5A LOAD IMPROVEMENT CONTROL SYSTEM (LICS)

Albert J. Van Dierendonck, et al

Honeywell, Incorporated

Prepared for:

Air Force Flight Dynamics Laboratory

October 1973

NOTICE

When Government drawings, specifications, or other data are used for any purpose other than in connection with a definitely related Government procurement operation, the United States Government thereby incurs no responsibility nor any obligation whatsoever; and the fact that the government may have formulated, furnished, or in any way supplied the said drawings, specifications, or other data, is not to be regarded by implication or otherwise as in any manner licensing the holder or any other person or corporation, or conveying any rights or permission to manufacture, use, or sell any patented invention that may in any way be related thereto.

Copies of this report should not be returned unless return is required by security considerations, contractual obligations, or notice on a specific document.

AD 776297

Security Classification

DOCUMENT CONTROL DATA - R & D

(Security classification of title, body of abstract and indexing annotation must be entered when the overall report is classified)

1 ORIGINATING ACTIVITY (Corporate author) Honeywell Inc. Systems and Research Division Minneapolis, Minnesota 55413	2a. REPORT SECURITY CLASSIFICATION Unclassified 2b. GROUP NA

3 REPORT TITLE

APPLICATION OF PRACTICAL OPTIMAL CONTROL THEORY TO THE C-5A LOAD IMPROVEMENT CONTROL SYSTEM (LICS)

4 DESCRIPTIVE NOTES (Type of report and inclusive dates)

Final Technical Report, 15 August 1972 - 15 September 1972

5 AUTHOR(S) (First name, middle initial, last name)

Albert J. VanDierendonck
Charles R. Stone
Michael D. Ward

6 REPORT DATE October 1973	7a. TOTAL NO. OF PAGES 45	7b. NO. OF REFS 6
8a. CONTRACT OR GRANT NO. F33615-72-C-2008 b. PROJECT NO. 487T0105 c. d.	9a. ORIGINATOR'S REPORT NUMBER(S) F0161-FR, Vol. III 9b. OTHER REPORT NO(S) (Any other numbers that may be assigned this report) AFFDL-TR-73-122	

10 DISTRIBUTION STATEMENT

"Approved for public release; distribution unlimited"

11 SUPPLEMENTARY NOTES	12 SPONSORING MILITARY ACTIVITY Air Force Flight Dynamics Laboratory Air Force Systems Command Wright-Patterson Air Force Base, Ohio

13 ABSTRACT

Practicalizing quadratic optimal control algorithms were used to design load relief systems for the C-5A, a large flexible aircraft. The predicted rms stresses at the wing root were reduced by more than 40 percent. Handling qualities or stability were not compromised. The control is realized with a gyro and three accelerometers affecting ailerons and elevator - two accelerometers more than an existing stability augmentation system. The quadratic performance index is defined to enforce good handling qualities and to limit the control system bandwidth.

ia

DD FORM 1 NOV 68 1473

Security Classification

Security Classification

14 KEY WORDS	LINK A		LINK B		LINK C	
	ROLE	WT	ROLE	WT	ROLE	WT
Lockheed C-5A						
Optimal Control						
Maneuver Load Control						
Wing Root Stress Reductions						
Practical Optimal Control						

ib

*U.S.Government Printing Office: 1974 — 758-432/426

APPLICATION OF PRACTICAL OPTIMAL CONTROL THEORY TO THE C-5A LOAD IMPROVEMENT CONTROL SYSTEM (LICS)

A. J. VAN DIERENDONCK
C. R. STONE
M. D. WARD

ic

FOREWORD

The technical work reported was conducted by the Research Department of the Systems and Research Center of Honeywell Inc., Minneapolis, Minnesota. The principal investigator was Dr. A. J. VanDierendonck. He was assisted by Mr. C.R. Stone and Mr. M.D. Ward. Dr. F.E. Yore was Program Manager at Honeywell. The Project Engineers were Major B. Kujawski (AFFDL/FGB) and Mr. Charles Stockdale. Their help is gratefully acknowledged.

This work was performed under Project No. 487T0105, Contract No. F33615-72-C-2008, sponsored by the Air Force Flight Dynamics Laboratory. The period of performance was from 15 August 1972 to 15 September 1972.

This work has benefited considerably from the past efforts of the author's colleagues at Honeywell. They are too numerous to be individually mentioned.

The manuscript was released by the authors in September 1973. The number assigned to this report by Honeywell Systems and Research Center is F0161-FR, Volume III.

This report has been reviewed and is approved.

Robert P. Johannes

Robert P. Johannes, Program Manager
Control Configured Vehicles
Flight Control Division

ABSTRACT

Practicalizing quadratic optimal control algorithms were used to design load relief systems for the C-5A, a large flexible aircraft. The predicted rms stresses at the wing root were reduced by more than 40 percent. Handling qualities or stability were not compromised. The control is realized with a gyro and three accelerometers affecting ailerons and elevator -- two accelerometers more than an existing stability augmentation system. The quadratic performance index is defined to enforce good handling qualities and to limit the control system bandwidth.

TABLE OF CONTENTS

		Page
SECTION I	INTRODUCTION AND SUMMARY	1
SECTION II	PROBLEM FORMULATION	3
	Design Procedure	3
	Control Law	4
	Performance Index	4
	The Problem	4
	Aircraft Model	5
	Response Selection	11
SECTION III	OPTIMAL STATE FEEDBACK CONTROL	13
SECTION IV	SIMPLIFIED FEEDBACK CONTROL	18
SECTION V	LICS FUNCTIONAL BLOCK DIAGRAMS	26
SECTION VI	CONCLUSIONS AND RECOMMENDATIONS	30
APPENDIX	SYSTEM MATRICES FOR FLIGHT CONDITION 37	31
REFERENCES		37

LIST OF ILLUSTRATIONS

		Page
1	The Lockheed C-5A	7
2	C-5A LICS Sensor Locations	9
3	Chronological Weighting of Responses for Optimal State Feedback Control Design	14
4	Chronological Stress Responses for Optimal State Feedback Control Design	14
5	Chronological Model-Following Responses for Optimal State Feedback Control Design	15
6	Aileron and Elevator Responses for Optimal State Feedback Control Design	15
7	Incremental Gradient for C-5A Design	23
8	Simplified Control Block Diagram (Controller 14C)	27
9	System I LICS (Without Spoilers) Block Diagram	28
10	System II LICS (With Spoilers) Block Diagram	29

LIST OF TABLES

I	Wing Root Stress Relief Summary	1
II	Comparison of RMS Responses Due to 1-FPS RMS Gust	10
III	Chronological Frequencies, Damping Ratios, and Actuator Roots for Optimal State Feedback Control Design	16
IV	Practical Design Results Summary	19
V	Design Results Summary with Six-Mode Model	20
VI	Spoiler Effectiveness for Gust Relief	20
VII	Candidate Measurement for Practical Designs	21
VIII	Maneuver Load Control	25

LIST OF SYMBOLS

VECTORS

x	State vector
u	Control vector
y	Measurement vector
r	Response vector
η	Disturbance vector
F_{1m}, F_{2m}	Row vectors of stability matrix of model-following model

MATRICES

F	System stability matrix
G_1	Control input matrix
G_2	Disturbance input matrix
H	Response state output matrix
D	Response control output matrix
M	Measurement output matrix
K^*	Measurement gains matrix
K	State gains matrix
Q	Quadratic weighting matrix

VARIABLES

J	Performance index
w	Vertical velocity
$\dot{\theta}/n_2$	Normalized pitch rate

VARIABLES (continued)

η_i	Bending-mode coordinate
δ_e	Elevator displacement
δ_a	Aileron displacement
δ_s	Spoiler displacement
s	Stress
$\dot{\theta}_L$	Lagged gyro output
a_L	Lagged accelerometer output
w_g	Gust vertical velocity
p	Wind model state
ω	Frequency
ζ	Damping ratio
$\dot{\theta}/n_2$	Model-following error
a	Acceleration
E	Expectation operator
Tr	Trace operator
λ	Gradient incrementing parameter

SUBSCRIPTS AND SUPERSCRIPTS

$(\dot{})$	Time derivative
$(\,)_m$	Model parameter
$(\,)^T$	Transpose of a vector or matrix
$(\,)_{sp}$	Short period
i	Inner surface
o	Outer surface
ℓ	Left
r	Right

SECTION I
INTRODUCTION AND SUMMARY

Quadratic methodology was applied to the design of a pitch-axis load-relief control system for the C-5A aircraft. Predicted rms stresses due to wind gusts at the wing root were reduced by 50 percent, while stress rates were reduced by 31 percent. This was done without serious degradation of the handling qualitities or the stability of the aircraft. Similar reductions in peak and steady-state stresses due to maneuvers were realized. Symmetric ailerons and the inboard elevator are driven by control signals from accelerometers and a gyro. One accelerometer and the gyro already exist in the stability augmentation system (SAS). The additional load improvement control system (LICS) accelerometers would be placed on outer wing panels.

The effectiveness of active control for effecting load improvement is summarized in Table I. Results are given for two systems. System I uses ailerons to reduce the loads, whereas System II uses spoilers in addition to

Table I. Wing Root Stress Relief Summary

Parameter	Ratio of Controlled Aircraft to Free Aircraft	
	System I: Ailerons, One Extra Sensor Set	System II: Ailerons + Spoilers, Two Extra Sensor Sets[c]
Wing root stress[a]	0.50	0.22
Wing root stress rate[a]	0.69	0.58
Peak maneuvering stress[a,b]	0.57	0.36
Steady-state maneuvering stress[a,b]	0.57	0.34

[a]For Lockheed flight condition 37 (w = 593,154 lb; M = 0.533; h = 10,000 ft) using a six-flexure-mode representation.

[b]For +1.5 incremental g using 25 deg of up aileron. The ailerons would hit the down stops of 15 deg at -0.9 incremental load factor.

[c]For 10 deg of up spoiler at +1.5 incremental g.

the ailerons. Table I shows that rms stress and stress rate can be reduced by 50 percent and 31 percent, respectively, using System I. Peak and steady-state maneuvering stresses can be reduced by 43 percent of their nominally attained values using System I. System I requires one additional set of sensors to achieve the gust relief improvements cited. In the study conducted, virtually no improvement was obtained using additional sensors.

By using spoilers, performance could be improved as indicated for System II in Table I. For System II, use of a pilot-operated switch is recommended to activate the spoiler portion of the system. In normal use the spoilers would not be deflected; the performance would be that of System I. In rough air, the spoilers would be activated to achieve the results noted for System II. The spoilers would be biased at 10 degrees in this mode of operation.

SECTION II
PROBLEM FORMULATION

DESIGN PROCEDURE

The design approach used is based on quadratic optimal control theory -- optimal with respect to a quadratic performance index subject to practical constraints. The background for this methodology is given in References 1 and 2.

The design is accomplished by minimizing a quadratic performance index which weights mean square stresses, stress rates, model-following errors, control surface rates and control surface deflections. Simple compensation filters were included in the measurement constraints to improved bending-mode damping and handling qualities. The model-following errors were weighted to enforce good handling qualities.

The quadratic optimal design technique requires that the aircraft be modeled as a linear time-invariant plant representing a single flight condition:

$$\dot{x} = Fx + G_1 u + G_2 \eta \tag{1}$$

$$r = Hx + Du \tag{2}$$

$$y = Mx \tag{3}$$

where

x = State vector (including rigid-body states, actuator and servo states, flexure-mode states, sensor states, model-following states, and wind states)

u = Control input vector

η = Unit-variance white noise vector

r = Response vector

y = Measurement vector

CONTROL LAW

The control law is constrained to be of the feedback gain form

$$u = K^* y \tag{4}$$

where the asterisk is used to differentiate this matrix K^* from the optimal full-state feedback form

$$u = Kx \tag{5}$$

PERFORMANCE INDEX

The performance index is defined to be

$$J = E\{Tr[Q\, r\, r^T]\} \tag{6}$$

THE PROBLEM

Using Equations (1) through (6), the problem reduces to minimizing the performance index J with respect to the gains matrix K^* subject to the constraint of system stability and Equations (1), (2), and (3).

There are two parts to this problem. This first part involves determining the full-state feedback [Equation (5)]. The second part involves constraining the feedback [Equation (4)] and is also known as the fixed-form optimal control problem. The first part of the problem is discussed in Section III. The simplified control law is discussed in Section IV.

AIRCRAFT MODEL

The design approach was applied to the pitch axis of the C-5A aircraft at one flight condition (FC-37) which is a low-altitude cruise condition with the following parameters:

- Gross weight - 593,154 lb (50% fuel, 50% cargo)
- Mach number - 0.533
- Altitude - 10,000 ft
- Dynamic pressure - 292 psf
- True airspeed - 577 fps
- Center-of-gravity location - 31% MAC

The general arrangement of the C-5A is shown in Figure 1. The spoilers being considered are the outboard spoilers (which consist of three panels). Figure 2 shows the locations of the sensors that will be considered in the control synthesis.

The procedure described in Reference 3 was used to reduce a C-5A model to the form of Equation (1). The procedure included the quasi-elastic effects of bending modes neglected, as only the three most prominent modes were included in the design. The final designs were checked using a six-mode model.

The Lockheed data (listed in Ref. 4) for FC-37 were processed by the computer programs developed for a con[illegible]-configured vehicle (CCV) (Ref. 3). Satisfactory agreement with load alleviation and mode stabilization (LAMS) results (Ref. 5) was not achieved. Two errors in the processing program (Table II-13 of Vol. II of Ref. 3) were found. After making these corrections, the results shown in Table II were obtained. Agreement is now considered to be sufficient for the intended purposes.

The notation used for column headings in Table II (e.g., LAMS-6) refers to the data source [LAMS (Ref. 5) or this contract] and the number of bending modes used. The number n_2 (shown in row 2) is used to convert $\dot{\theta}$ from rad/sec to in/sec. It is equal to 0.6066×10^{-3}.

The state vector, x, for optimal state feedback designs was (17 states):

$$x^T = (w,\ \dot{\theta}/n_2,\ \dot{\eta}_1,\ \dot{\eta}_6,\ \dot{\eta}_3,\ \eta_1,\ \eta_6,\ \eta_3,\ \delta_a,\ \delta_e,\ p_1,\ p_2,\ p_3,\ p_4,\ p_5,\ p_6,\ w_g) \tag{7}$$

where w is the rigid-body vertical velocity (in./sec), $\dot{\theta}/n_2$ is a normalized rigid-body pitch rate, η_1 is the first bending-mode coordinate, η_6 is the sixth bending-mode coordinate, η_3 is the third-mode coordinate, δ_a is symmetric aileron displacement, δ_e is the inboard elevator displacement, p_1 through p_6 are wind distribution and lift growth states, and w_g is the vertical gust velocity.

The control input vector, u, contains the inputs to the actuator models (two controls):

$$\begin{aligned} \dot{\delta}_a &= -6\,\delta_a + 6\,u_{\delta_a} \\ \dot{\delta}_e &= -6\,\delta_e + 6\,u_{\delta_e} \end{aligned} \tag{8}$$

BASIC DATA	WING	VERTICAL	HORIZONTAL
AREA, SQ FT	6200 •	961.067	965.824
ASPECT RATIO	7.75 •	1.24	4.74
TAPER RATIO	0.371 •	0.600	0.370
SWEEP AT 25% CHORD	25° ●	34°56'	24°35'
ROOT CHORD, IN.	545.303	371.197	250.160
CHORD PLANFORM BREAK	335.366	——	——
TIP CHORD, IN.	184.036	296.958	92.659
MAC, IN. (PROJECTED)	370.523•	335.452	183.438
AERODYNAMIC SPAN, IN.	2630.437	414.256	811.620
ANHEDRAL	5°5'32"••	——	5°0'
INCIDENCE	3°30'•••	——	+4° TO -12°

WEIGHT •	
CONDITION	LB
EMPTY	~~318,469~~ ← 319,809 (SCN 7-1-34)
DESIGN FLIGHT GROSS (2.5g)	728,000
USEFUL LOAD - DESIGN FLIGHT	409,531
MAXIMUM DESIGN GROSS	769,000
USEFUL LOAD - MAXIMUM DESIGN	450,531

● (TRUE MAC • 371.209) (REF)
● SWEEP OF OUTER WING IN ROOT CHORD PLANE
• IN AERODYNAMIC PLANE
••IN AIRPLANE FRONT VIEW, 3° 30' 0" AROUND ROOT CHORD
•••ROOT CHORD

● GUARANTEE FIGURES

(4) TF39 ENGINES

MISCELLANEOUS DATA		AILERON	SPOILERS	TRAILING EDGE FLAPS	LEADING EDGE SLATS	ELEVATOR	RUDDER
AREA SQ FT	INBOARD	——	218.128	493.407	◐ 322.348	180.159	UPPER-99.584
	MIDDLE	——	72.500 △	161.576 □	◒ 99.147	——	——
	OUTBOARD	252.782	140.004 ▲	336.799	◒ 227.044	78.515	LOWER-127.076
	TOTAL/SIDE	126.396	215.366 ●	495.691	324.269	129.337	TOTAL-226660
DEFLECTION		UP 25° DOWN 15°	GRD 60° FLT 22.5°	TAKE-OFF 25° LANDING 40°	SEALED 21.5° SLOTTED 22°	UP 25° DOWN 15°	±35°

△ACROSS WING BREAK (LATERAL CONTROL)
▲OUTBOARD WING (LATERAL CONTROL)
●ALL SPOILERS (GROUND OPERATION)
□ ACROSS WING BREAK
◐ INBOARD WING (SEALED)
◒ WING BREAK TO OUTBOARD ENGINE (SEALED)
◓ OUTBOARD ENGINE TO WING TIP (SLOTTED)

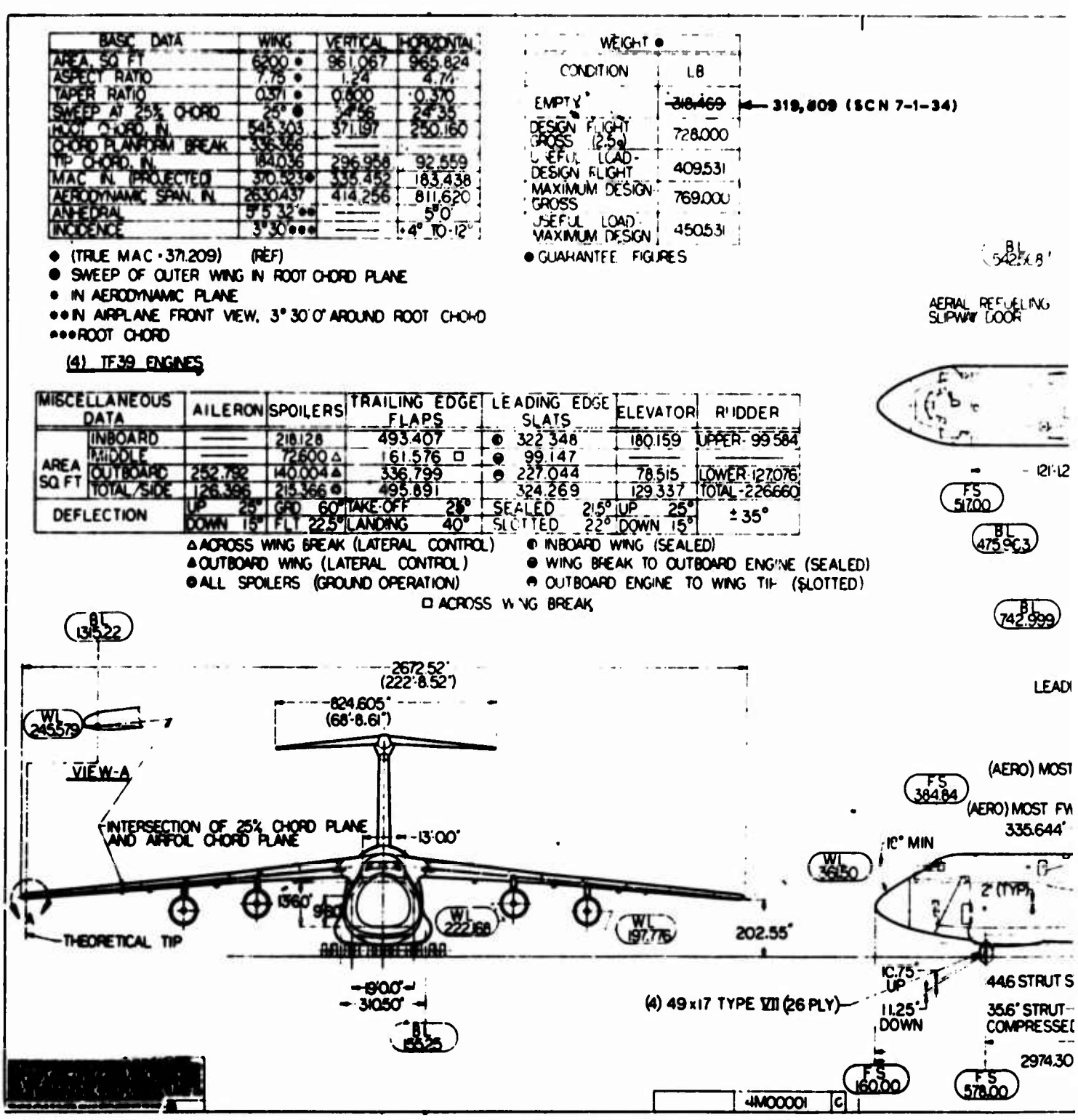

Figure 1. The Lo

A

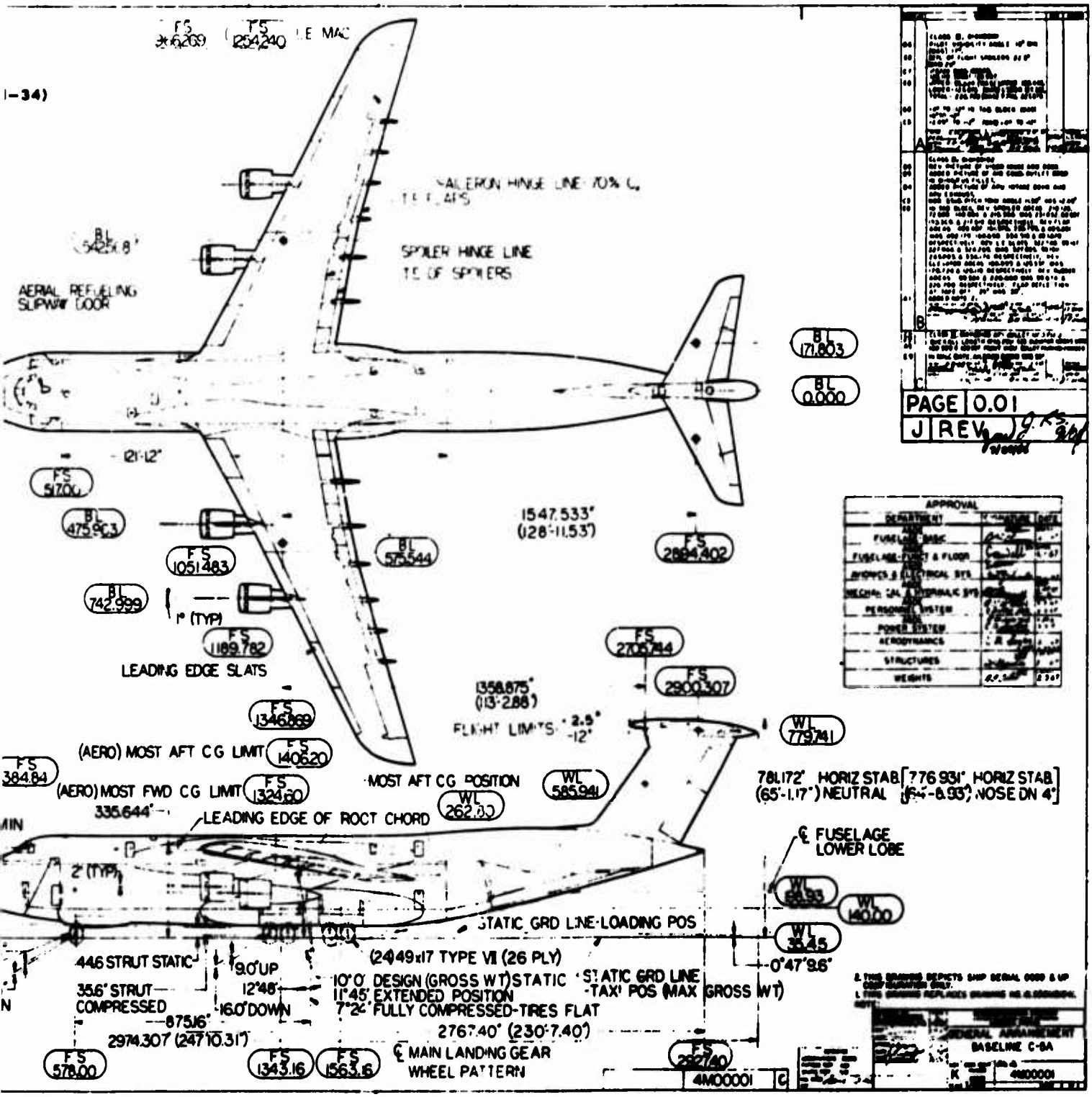

ure 1. The Lockheed C-5A

B

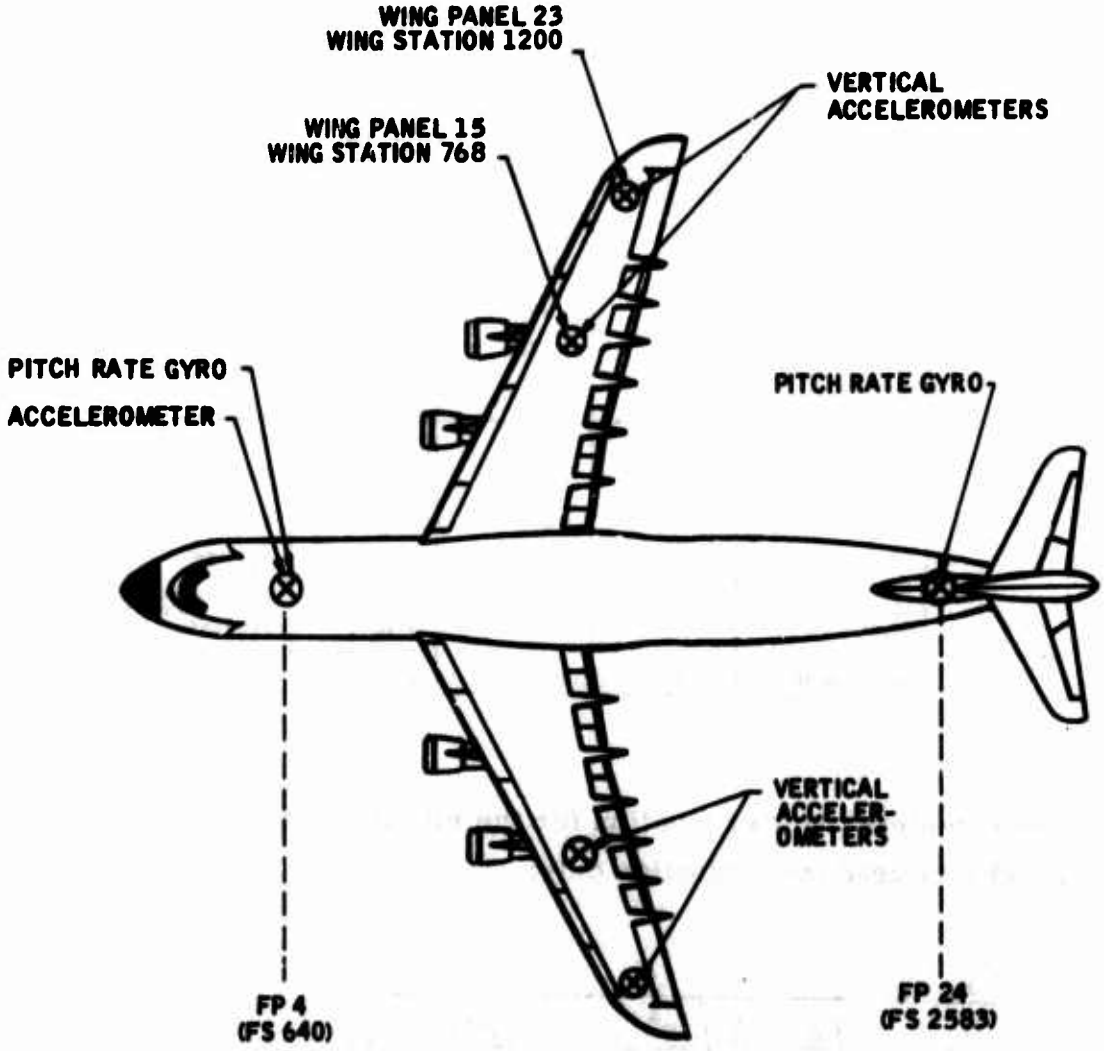

Figure 2. C-5A LICS Sensor Locations

Table II. Comparison of RMS Responses Due to 1-FPS RMS Gust

Parameter	LAMS-6	LAMS-15	LICS-3	LICS-6
w (in/sec)	10.42	---	11.08	11.03
$\dot{\theta}/n_2$ (in/sec)	1.48	---	1.12	1.123
η_1 (in.)	0.421	---	0.549	0.550
$\dot{\eta}_1$ (in/sec)	1.61	---	1.932	1.94
η_3 (in.)	0.0332	---	0.0331	0.0339
$\dot{\eta}_3$ (in/sec)	0.382	---	0.314	0.329
η_6 (in.)	0.01268	---	0.0096	0.00968
$\dot{\eta}_6$ (in/sec)	0.1462	---	0.0411	0.0456
s_1 (psi)	138.8	22^ 4	178.0	179.0
$\dot{s}_1$ (psi/sec)	532.4	1040.0	571.0	564.0
s_2 (psi)	143.5	243.1	183.8	181.0
$\dot{s}_2$ (psi/sec)	853.7	1576.0	841.0	870.0
No. of modes	6	15	3	6
Modes used	1,3,4,6, 7,11	All	1,3,6	1,2,3,4,5,6
Gust penetration	No	Yes	Yes	Yes
Wagner dynamics	Constant (unity)	Second-order	Constant (unity)	Constant (unity)
Mode approximation	Truncated	Completed	Steady-state retained	Steed-state retained
Scale length (ft)	1000	1000	1750	1750

The complete transfer function for the elevator and aileron is third-order and was used for evaluation only:

$$\frac{\delta_a}{u_{\delta_a}} = \frac{1}{\left(\frac{s}{6}+1\right)\left(\frac{s^2}{(65)^2}+\frac{0.32s}{65}+1\right)}$$

$$\frac{\delta_e}{u_{\delta_e}} = \frac{1}{\left(\frac{s}{7.5}+1\right)\left(\frac{s^2}{(75)^2}+\frac{0.28s}{75}+1\right)} \qquad (9)$$

RESPONSE SELECTION

The objective of the LICS design was to significantly reduce wing root stress and stress rate using active control without degrading the existing handling qualities. This reduction was to consider both maneuvering relief as well as gust-induced stresses. Therefore, the response vector, r, minimized was

$$r^T = (s_1, s_2, \dot{s}_1, \dot{s}_2, \dot{\delta}_a, \dot{\delta}_e, \delta_a, \delta_e, \dot{\theta}/n_2) \tag{10}$$

where s_1 is the stress at the wing root, s_2 is the stress at a mid-wing panel, and $\dot{\theta}/n_2$ is a model-following error. The model-following error represents the difference between the pitching moment equation of the aircraft and a rigid model with desired handling qualities. That is,

$$\dot{\theta}/n_2 = (F_2 - F_{2m})\, x \tag{11}$$

where F_2 is the second row of the stability matrix F of the aircraft and F_{2m} is the second row of the stability matrix of the model. This row is given by

$$F_{2m} = (F_{21m}, F_{22m}, 0, \ldots, 0, F_{2,11}, \cdots, F_{2,17}) \tag{12}$$

Here, F_{21m} and F_{22m} are selected so that the desired short-period frequency and damping ratio are computed from

$$\omega_{sp}^2 = F_{11}F_{22m} - F_{21m}F_{12} \tag{13}$$

$$2\zeta_{sp}\omega_{sp} = -F_{11} - F_{22m} \tag{14}$$

where F_{11} and F_{12} are elements of the first row of F. This is because the z force (row 1 of the model) is taken to be

$$F_{1m} = (F_{11}, F_{12}, 0, \ldots, 0, F_{1,11}, \ldots, F_{1,17}) \tag{15}$$

The wind coefficients of the model are taken to be the same as the aircraft itself. The wind coefficients of the model in Equation (12) should probably be adjusted to agree with an adjustment in F_{21m}, the coefficient of w. However, in this design, F_{21m} and F_{22m} are the same as F_{21} and F_{22}. Thus, the model-following error tends only to decouple the bending modes from the rigid body.

The matrices of Equation (1), (2), and (3) corresponding to this flight condition are tabulated in the Appendix.

SECTION III
OPTIMAL STATE FEEDBACK CONTROL

Optimal full-state feedback designs were obtained for various quadratic weighting selections on the responses of Equation (10). Not all responses were weighted; some were only monitored to ensure that they were not compromised. This was especially true with s_2 and $\dot{s}_2$, the mid-wing stress and stress rate.

The quadratic weights selected versus chronological designs are shown in Figure 3. Zero weights are not shown. The weights on $\dot{\delta}_e$ and $\dot{\bar{\theta}}/n_2$ are not shown, since they were held constant at 20 and 10^{-4}, respectively. These weights, as well as the initial weights (iteration 1), were determined in previous designs with erroneous stress equations. The weights on $\dot{\delta}_e$ and $\dot{\bar{\theta}}/n_2$ were iteratively selected to constrain the rigid-body frequency and damping ratio. This was done with relatively little effect on stress control. Figures 4, 5, and 6 present the root mean square (rms) responses and rigid-body frequencies and damping ratios corresponding to the weights of Figure 3. The dashed lines represent responses which are not weighted. Table III lists the corresponding frequencies, damping ratios, and actuator root locations of 14 optimal (full-state feedback) control designs. The rationale used in the designs will now be discussed.

On iteration 1, the aileron actuator root was large (caused by a significant negative feedback of δ_a to u_{δ_a}). Thus, the aileron rate weight, $Q_{\dot{\delta}_a}$, was increased for iteration 2. There was a corresponding increase in stress s_1. In an attempt to simultaneously decrease δ_a feedback and increase aileron effectiveness, the weight on aileron displacement, Q_{δ_a}, was removed for iteration 3. This had very little effect. Thus, for iteration 4, this weight was reinstated and the aileron rate weight, $Q_{\dot{\delta}_a}$, was increased further. The aileron feedback became positive and the stress increased; so, on the fifth iteration, the $Q_{\dot{\delta}_a}$ weight was cut in half.

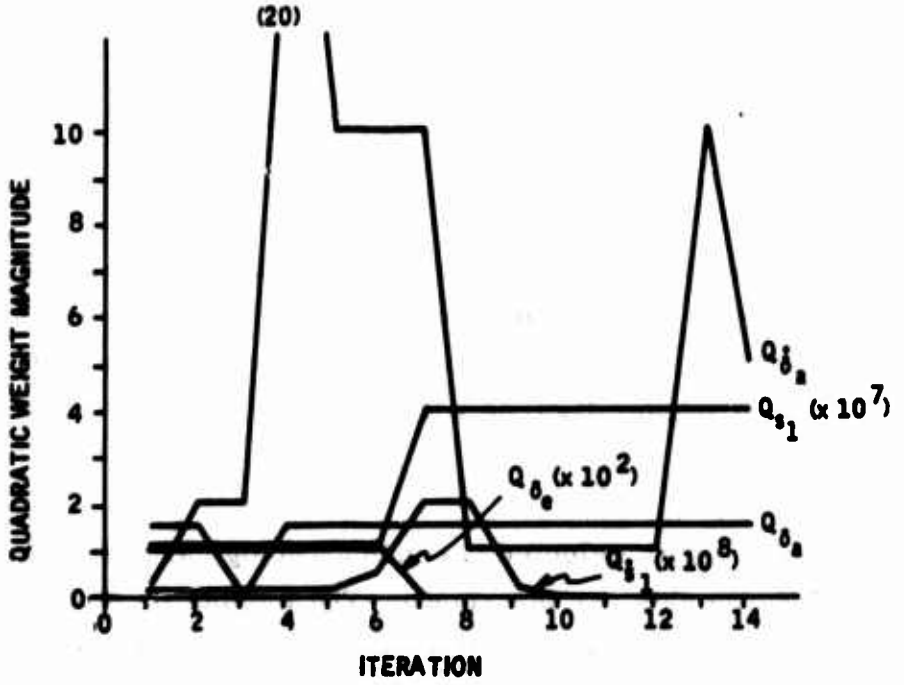

Figure 3. Chronological Weighting of Responses for Optimal State Feedback Control Design

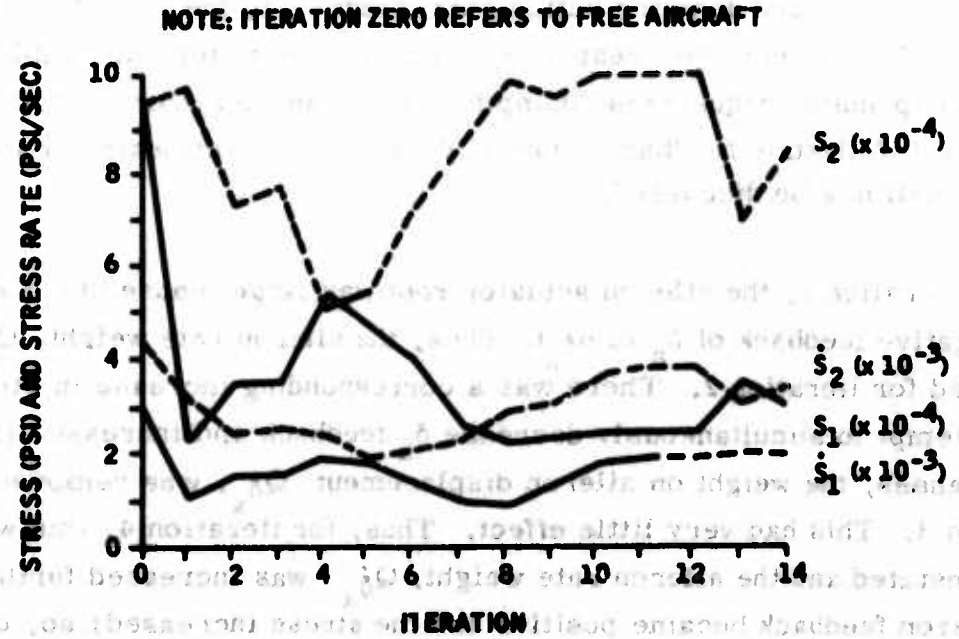

Figure 4. Chronological Stress Responses for Optimal State Feedback Control Design

NOTE: ITERATION ZERO REFERS TO FREE AIRCRAFT

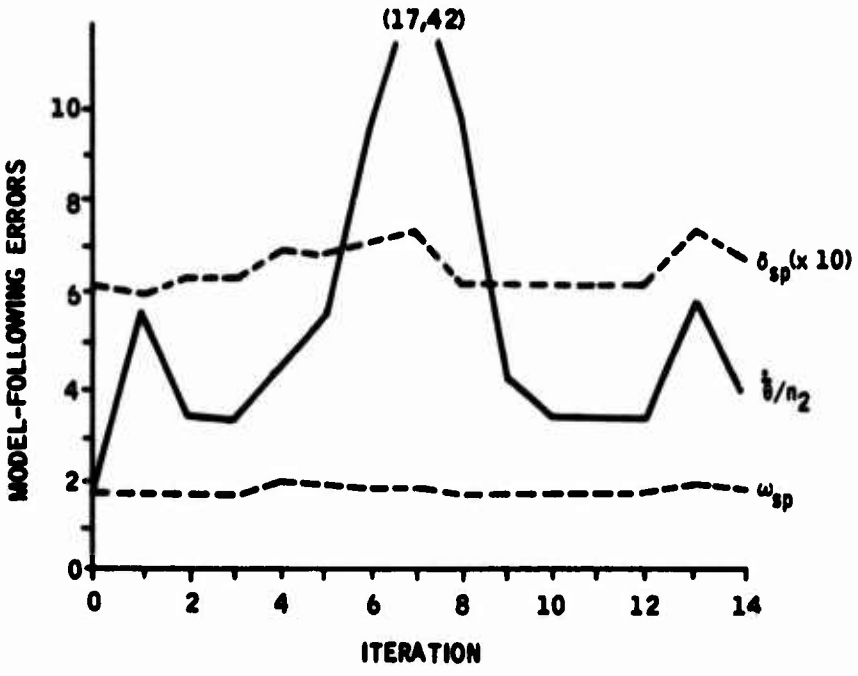

Figure 5. Chronological Model-Following Responses for Optimal State Feedback Control Design

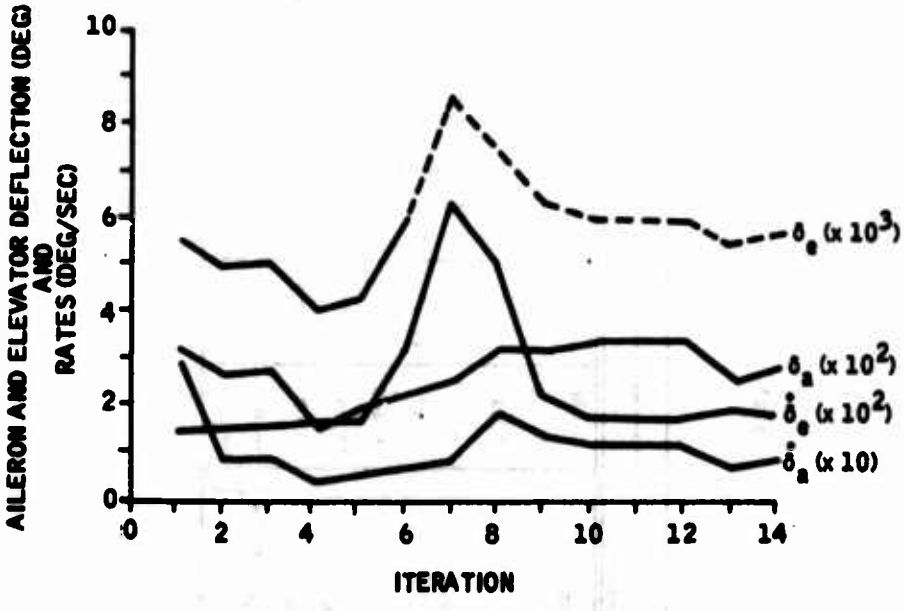

Figure 6. Aileron and Elevator Responses for Optimal State Feedback Control Design

Table III. Chronological Frequencies, Damping Ratios, and Actuator Roots for Optimal State Feedback Control Design

Parameter	Iteration														
	0	1	2	3	4	5	6	7	8	9	10	11	12	13	14
ω_{sp}	1.688	1.66	1.69	1.67	1.94	1.88	1.78	1.78	1.67	1.66	1.67	1.67	1.67	1.83	1.72
ζ_{sp}	0.614	0.60	0.63	0.63	0.69	0.68	0.71	0.73	0.62	0.614	0.614	0.614	0.615	0.73	0.67
ω_1	5.73	7.35	7.06	7.06	6.06	6.29	7.10	8.00	11.27	8.23	7.87	7.88	7.88	6.56	6.93
ζ_1	0.1700	0.78	0.565	0.564	0.322	0.39	0.582	0.75	0.87	0.70	0.510	0.49	0.49	0.326	0.374
ω_3	14.49	17.06	15.2	15.2	14.46	14.57	14.86	15.28	19.67	16.36	14.90	14.78	14.77	14.50	14.54
ζ_3	0.049	0.379	0.160	0.160	0.069	0.103	0.170	0.25	0.42	0.23	0.1222	0.106	0.104	0.060	0.069
ω_6	19.36	18.61	19.37	19.37	19.46	19.45	19.69	20.07	18.80	19.21	19.36	19.36	19.36	19.36	19.36
ζ_6	0.064	0.064	0.047	0.047	0.042	0.042	0.060	0.06	0.07	0.059	0.0387	0.037	0.037	0.034	0.035
δ_a, δ_e roots	-6.0	-48.5	-8.06	-8.03	-6.97	-1.37	-1.00	-1.28	-1.40	-9.17	-9.28	-9.28	-9.28	-2.47	-3.45
	-6.0	-2.82	-2.31	-2.25	-6.96	-6.96	-6.81	-6.43	-6.71	-3.68	-4.77	-4.82	-4.82	-7.03	-7.28

The iteration 3 controller was quite acceptable, if the δ_a feedback could be successfully eliminated later during practicalization designs. Stress was reduced 67 percent on that iteration, and stress rate 50.5 percent. The iteration 5 controller is a compromise, with a 49.5-percent reduction in stress and a 42.3-percent reduction in stress rate.

In an attempt to reduce stress rate even more, the stress rate weight, $Q_{\dot{s}_1}$, was increased and Q_{δ_e} was removed for iteration 6. Both stress and stress rate decreased, with a significant increase in bending-mode damping, although the model-following error, short-period damping ratio, and δ_e feedback to u_{δ_e} increased somewhat. This controller was also considered a candidate for practical design; however, from past experience, it was expected to lead to difficulty. Generally, practical measurements cannot produce this much bending-mode damping without excessive filtering. This is especially true when slow actuators are used.

Iterations 7 through 11 were further attempts to reduce stress. Finally, by deemphasizing reductions in stress rate, stress could be reduced much more within the constraints of the actuator bandwidths. The stress rate weight, $Q_{\dot{s}_1}$, was removed by iteration 12. However, the δ_a feedback to u_{δ_a} was still high. Iterations 13 and 14 brought this feedback to within reason for practical design. The iteration 14 controller was also a candidate for practical design. With this controller, stress was reduced 67.8 percent and stress rate 36 percent, with small δ_a to u_{δ_a} feedback.

SECTION IV
SIMPLIFIED FEEDBACK CONTROL

This section summarizes the LICS control design effort. The first set of controllers used ailerons and elevator and was based on a three-mode model. Both full-state and measurement feedback were evaluated (Table IV). Three of the 14 full-state feedback controllers were successfully simplified.

The second set of controllers also used aileron and elevator but was based on a six-mode model. Both full-state and measurement feedback were evaluated (Table V).

The last set of controllers used spoilers and elevator with a three-mode model. Only full-state control was considered (Table VI).

With the iteration 3, 5, 6, and 14 controllers as baselines, practical designs were attempted using their respective quadratic weights and their optimal gains as starting points. The practical designs were attempted with different measurement complements. The candidate measurements are listed in Table VII.

For most of the practical designs, the state vector, x^T, included 18 states:

$$x^T = \left[w,\ \dot{\theta}/n_2,\ \dot{\eta}_1,\ \dot{\eta}_6,\ \dot{\eta}_3,\ \eta_1,\ \eta_6,\ \eta_3,\ \delta_a,\ \delta_e,\ \dot{\theta}_L,\right.$$
$$\left. p_1,\ p_2,\ p_3,\ p_4,\ p_5,\ p_6,\ w_g\right] \qquad (16)$$

Table IV. Practical Design Results Summary

Parameter	Controller											
	5	5A	5B	5C	5D	3	3A	3B	14	14A	14B	14C
s_1 ($\times 10^{-3}$)	0.467	0.561	0.569	0.570	0.556	0.341	0.457	0.504	0.296	0.453	0.456	0.449
$\dot{s}_1$ ($\times 10^{-3}$)	1.714	2.178	2.292	2.006	2.196	1.471	2.045	2.290	1.902	2.358	2.371	2.312
s_2 ($\times 10^{-3}$)	0.518	0.383	0.401	0.284	0.261	0.770	0.364	0.558	0.940	0.733	0.763	0.750
$\dot{s}_2$ ($\times 10^{-3}$)	1.78	2.480	2.713	2.634	2.481	2.421	2.513	2.615	3.257	2.844	3.008	2.882
δ_a	0.046	0.0422	0.0422	0.0385	0.0425	0.062	0.0619	0.0585	0.076	0.0648	0.0638	0.0661
δ_e	0.017	0.0124	0.0096	0.0136	0.0129	0.016	0.0131	0.0108	0.018	0.0156	0.0140	0.0146
$\dot{\delta}_a$	0.019	0.0162	0.0163	0.0128	0.0141	0.027	0.0190	0.0222	0.028	0.0256	0.0261	0.0296
$\dot{\delta}_e$	0.0044	0.0034	0.0033	0.0027	0.0030	0.0061	0.0036	0.0030	0.0057	0.0048	0.0048	0.0046
δ/n_2	5.47	5.415	4.229	6.263	5.244	3.28	3.606	3.286	3.67	6.214	6.055	6.103
ω_{sp}	1.82	3.60	1.965	1.783	1.980	1.67	1.765	1.768	1.72	2.432	2.483	2.008
ζ_{sp}	0.68	0.711	0.654	0.820	0.663	0.63	0.479	0.572	0.67	0.668	0.730	0.830
ω_1	6.20	5.54	5.58	5.866	5.971	7.08	6.336	5.49	6.93	5.754	5.682	6.106
ζ_1	0.30	0.158	0.180	0.158	0.213	0.564	0.137	0.191	0.374	0.150	0.151	0.218
ω_3	14.57	14.16	14.22	14.27	14.35	15.2	14.12	14.12	14.54	14.17	14.25	14.28
ζ_3	0.103	0.117	0.078	0.073	0.079	0.100	0.000	0.001	0.000	0.001	0.004	0.002
ω_6	19.45	19.37	19.37	19.70	20.04	19.37	19.61	19.41	19.36	19.37	19.38	19.35
ζ_6	0.042	0.022	0.025	0.013	0.031	0.047	0.000	0.023	0.035	0.020	0.017	0.025
δ_e, δ_a roots	-1.37	-1.53	-6.28	-5.25	-5.68	-8.03	-7.17	-6.67	-3.45	-5.87	-5.54	-3.01[c]
	-6.96	-7.26	±j1.79	-18.64	±j1.74	-2.25	-11.34	±j2.40	-7.28	±j2.26	±j1.43	±j2.01
δ_L root	---	-0.988	-0.849	-0.813	-0.862	---	-0.824	-0.839	---	-0.823	-0.833	-0.830
a_L root	---	---	---	---	---	---	---	---	---	---	---	-6.15[c]
Feedback to aileron[a, b]	All states	1,2,3	1,2	1,2,δ_a	1,2,5	All states	1,2,δ_a	1,2,4	All states	1,2,4	1,2,δ_a	1,6
Feedback to elevator[a, b]	All states	1,2,3,4	1,2,4	1,2,4,δ_a	1,2,4,5	All states	1,2,4,δ_a	1,2,4	All states	1,2,4	1,2,4,δ_a	1,4,6

[a] Measurements are defined in Table VII.

[b] δ_a denotes aileron position feedback.

[c] Compensation root merged with actuator root.

Table V. Design Results Summary with Six-Mode Model (σ_{wind} = 5.2 fps)

Parameter	Free Aircraft	Controller				
		1	2	3	4	5
s_1 (10^3 psi)	0.930	0.482	0.311	0.470	0.581	0.467
s_2 (10^3 psi)	0.940	0.580	0.943	0.873	0.520	0.887
$\dot{s}_1$ (10^3 psi/sec)	2.928	1.686	1.867	2.361	2.262	2.328
$\dot{s}_2$ (10^3 psi/sec)	1.527	2.467	3.579	3.127	2.928	3.010
w_{total} (fps)	43.78	42.20	43.00	36.43	36.78	36.83
$\dot{\theta}/n_z$ (in/sec)	5.85	5.60	5.62	4.55	5.15	4.35
$\dot{\delta}_a$ (rad/sec)	0	0.0468	0.0764	0.0671	0.0436	0.0068
$\dot{\delta}_e$ (rad/sec)	0	0.0150	0.0183	0.0164	0.0102	0.0154
δ_a (rad)	0	0.0188	0.0281	0.?255	0.01631	0.0266
δ_e (rad)	0	0.0045	0.0058	0.0048	0.0033	0.0047
Actuator model	---	1[a]	1[a]	3[b]	3[b]	3[b]
Feedbacks	None	All states	All states	Same as 5C of Table IV	Same as 5C of Table IV	Same as 5C of Table IV

[a]First-order model [Refer to Equation (8)].
[b]Third-order model [Refer to Equation (9)].

Table VI. Spoiler Effectiveness for Gust Relief (σ_{wind} = 5.2 fps)[a]

Parameter	Free Aircraft	State Control 1	State Control 2
s_1 (10^3 psi)	0.925	0.037	0.084
s_2 (10^3 psi)	0.951	0.321	0.511
$\dot{s}_1$ (10^3 psi/sec)	2.972	0.286	0.665
$\dot{s}_2$ (10^3 psi/sec)	4.380	0.944	1.407
w_{total} (fps)	37.84	43.94	42.27
$\dot{\theta}/n_z$ (in/sec)	5.81	7.25	6.83
$\dot{\delta}_a$ (rad/sec)	0	0.0056	0.054
$\dot{\delta}_e$ (rad/sec)	0	0.0138	0.0146
δ_a (rad)	0	0.0034	0.0166
δ_e (rad)	0	0.0058	0.0058
δ_s (rad)	0	0.036	0.0245
$\dot{\delta}_s$ (rad/sec)	0	0.094	0.0598

[a]Three-mode representation with first-order actuators, deflected spoiler system, state control.

Table VII. Candidate Measurement for Practical Designs

Measurement Number	Description
1	Accelerometer located at fuselage panel 4 (forward)
2	Difference between accelerometer located at fuselage panel 4 and average of accelerometers located at wing panels 23 (tip)
3	Difference between accelerometer located at fuselage panel 4 and average of accelerometers located at wing panels 15 (mid-wing)
4	Combination of lagged and highpassed rate gyro located at fuselage panel 4 (forward) with frequency cutoff at 0.88 rad/sec ($-Z_w$)
5	Rate gyro located at fuselage panel 24 (aft)
6	Lagged measurement 2 with frequency cutoff at 2 rad/sec

which is the same as Equation (7) with the addition of $\dot{\theta}_L$, the lagged fuselage panel 4 rate gyro output used to construct measurement 4 of Table VII. In the designs where the lagged acceleration measurement was used, the state vector included 19 states:

$$x^T = (w,\ \dot{\theta}/n_2,\ \dot{\eta}_1,\ \dot{\eta}_6,\ \dot{\eta}_3,\ \eta_1,\ \eta_6,\ \eta_3,\ \delta_a,\ \delta_e,\ \dot{\theta}_L,\ a_L,\ p_1,\ p_2,\ p_3,\ p_4,\ p_5,\ p_6,\ w_g) \tag{17}$$

where a_L is the lagged acceleration measurement.

The design procedure described in References 1 and 2 was used to realize the practical designs. Using this procedure, the measurement gains are written as a function of a scaler parameter, λ, such that

$$K^*(\lambda) = K^1(\lambda) + \lambda K^2 \qquad 0 \le \lambda \le 1 \tag{18}$$

The incrementing parameter, λ, is equal to 1 for the optimal state feedback controller, and λ is equal to zero for the optimal measurement feedback controller.

The starting point ($\lambda = 1$) is found by using the optimal state feedback gains and the measurement matrix (augmented with direct measurements of states not necessarily measurable so M^{-1} exists):

$$K^*(1) = KM^{-1} \tag{19}$$

The measurement constraints are applied gradually by stepping λ to zero. The matrix $K^1(0)$ is the fixed-form solution and has the gain structure desired.

This procedure of "backing off" from the state feedback controller is illustrated in Figure 7 for the design of controller 14C (defined below). The same quadratic performance index was minimized while the measurement constraints were gradually applied.

The cost J is minimized at each increment of λ, with respect to the gains on the measurements. The gains are predicted for each increment. The minimization of J is the correction. The differences between the gradient norms before and after the corrections are also shown in Figure 7.

The practical designs are summarized in Table IV, except for the practicalization of the iteration 6 controller. In an attempt to practicalize this controller using measurements 1, 2, 3, and 4, the rigid-body and first bending-mode frequencies and damping ratios became unacceptable, as their roots appeared to merge with actuator roots. The successful practical designs will now be discussed.

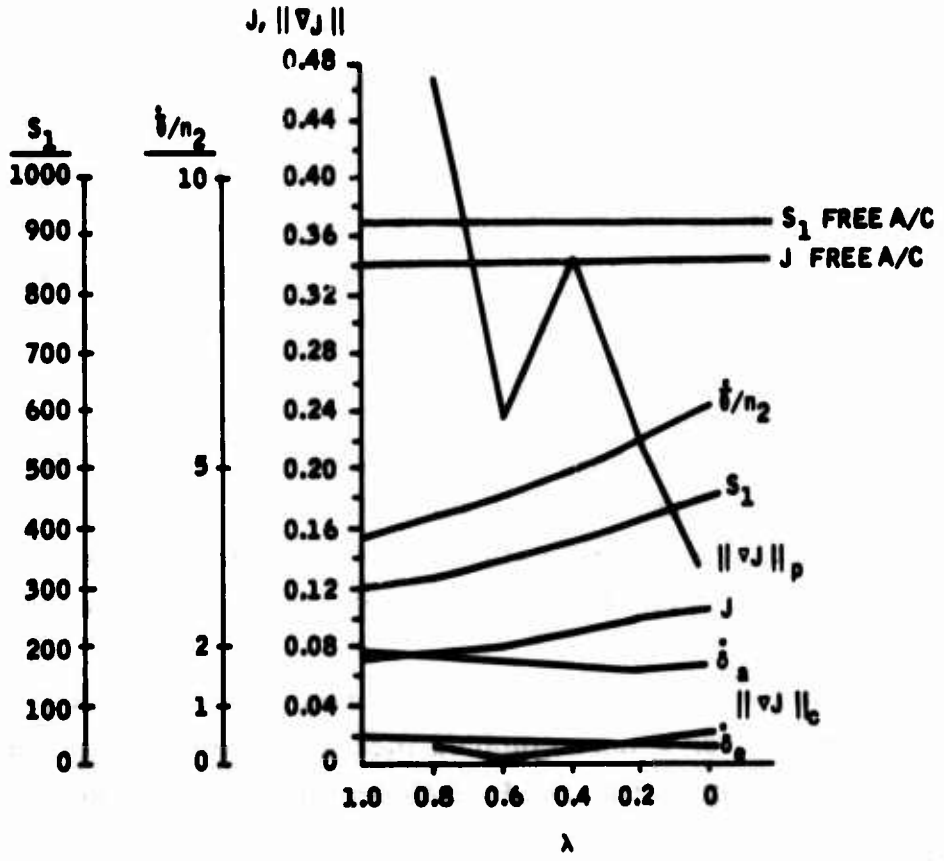

Figure 7. Incremental Gradient for C-5A Design

Successful designs were achieved using iteration 3, 5, and 14 controllers as baselines. Controller 5A had one more accelerometer measurement than 5B. This accelerometer gained very little stress and stress rate reduction at the expense of overcontrolling the rigid body. It slightly improved mode 3 damping, with less damping on modes 1 and 6. On controller 5C, aileron feedbacks were permitted. This defined a prefilter for the actuator. There was an improvement over 5B in stress rate and stress z_2 (not weighted) at the expense of bending-mode damping. The aft rate gyro was included in controller 5D, with some improvement over 5B in stress, stress rate, and mode damping.

Controllers 3A and 3B are based on the iteration 3 controller. On controller 3A, aileron feedbacks were allowed, with significant improvements in stress and stress rate at the expense of bending-mode damping.

Controller 14 practical controllers 14A, 14B, and 14C produced lower stress s_1 levels than the others. Stress rate levels were higher. On controller 14C, measurement 6 (lagged acceleration) increased bending-mode damping and lowered the short-period frequency. The short-period damping ratio was somewhat higher, however.

Controllers 5D, 3B, and 14C are the most desirable controllers from the bending-mode damping viewpoint, which could be important for stability margins. Controller 3B is the least complex of the three; however, 14 C is only different by a lag network. Controller 5D uses an extra sensor.

Table V summarizes the performance of two state-feedback and three practical controllers for a more complex model containing six bending modes. The results are not markedly different using a more complete model.

Table VI shows the effectiveness of spoiler controls in providing gust load relief. These are for state controls. Since full-state feedback was used, conservative depreciation was used from these answers to provide the numbers of Table I representing the results of simplified control.

Table VIII presents results for maneuvering load control (MLC). The maneuver is a step column input that attains a steady-state value of 1.5 incremental g.

The free aircraft does not use symmetric ailerons in the steady state. At +1.5 incremental g, the wing root perturbation stress is -17,400 psi. The peak perturbation stress achieved during the transient for the step column input is -18,700 psi (row 1 of Table VIII).

Controllers 3A and 3B are based on the iteration 3 controller. On controller 3A, aileron feedbacks were allowed, with significant improvements in stress and stress rate at the expense of bending-mode damping.

Controller 14 practical controllers 14A, 14B, and 14C produced lower stress s_1 levels than the others. Stress rate levels were higher. On controller 14C, measurement 6 (lagged acceleration) increased bending-mode damping and lowered the short-period frequency. The short-period damping ratio was somewhat higher, however.

Controllers 5D, 3B, and 14C are the most desirable controllers from the bending-mode damping viewpoint, which could be important for stability margins. Controller 3B is the least complex of the three; however, 14 C is only different by a lag network. Controller 5D uses an extra sensor.

Table V summarizes the performance of two state-feedback and three practical controllers for a more complex model containing six bending modes. The results are not markedly different using a more complete model.

Table VI shows the effectiveness of spoiler controls in providing gust load relief. These are for state controls. Since full-state feedback was used, conservative depreciation was used from these answers to provide the numbers of Table I representing the results of simplified control.

Table VIII presents results for maneuvering load control (MLC). The maneuver is a step column input that attains a steady-state value of 1.5 incremental g.

The free aircraft does not use symmetric ailerons in the steady state. At +1.5 incremental g, the wing root perturbation stress is -17,400 psi. The peak perturbation stress achieved during the transient for the step column input is -18,700 psi (row 1 of Table VIII).

Table VIII. Maneuver Load Control[a]

s_1 Steady-State (10^3 psi)	s_1 Peak (10^3 psi)	δ_a Steady-State (deg)	δ_{sc} Steady-State (deg)	Remarks
-17.4	-18.7	0	0	Free aircraft
- 9.81	-13.1	-25	0	Free aircraft
- 6.27	- 8.66	-25	-10	Free aircraft
- 9.81	-10.6	-25	0	With feedback

[a]For +1.5 incremental-g command. Relief is linear with control. Hence, results may be used to determine effectiveness with different surface deflections.

The effects of connecting the input of the aileron actuator to the control column are shown in row 2 of Table VIII. Steady-state values at 1.5 perturbation g of s_1 and δ_u are -9810 psi and 25 deg. Thus, the steady-state MLC relief is $1 - \frac{9810}{17,400} = 0.4362$. The ratio of peak stresses without and with MLC for the free aircraft is $1 - \frac{12,100}{18,700} = 0.3529$.

Table VIII (row 3) shows that adding the spoiler to the free aircraft provides further reductions in both steady and peak wing root stresses.

Table VIII (row 4) shows that feedback provides attenuation of peak maneuvering stresses; but, of course, it can do no better than the free aircraft (with MLC ailerons) in the steady state at +1.5 incremental g.

SECTION V
LICS FUNCTIONAL BLOCK DIAGRAMS

The block diagram corresponding to simplified controller 14C (Table IV) is shown in Figure 8. The MLC feedforward gain was computed to enforce the appropriate steady-state aileron surface deflection per g. At a single flight condition this was satisfactory. However, flight throughout the envelope would have required excessively complex scheduling because of the large variation in control column deflection per g with center-of-gravity variations. The system was then revised to provide maneuvering relief with a feedback control (Figure 9) using the inputs to the aileron and elevator servos. The only feedforwards remaining are the existing mechanical links in the aircraft. Gains and time constants were not determined for this configuration.

Similarly, Figure 10 illustrates a possible functional block diagram of a system using the spoilers in addition to the aileron and elevator. The various gains shown were not determined.

System I (Figure 9) requires one additional pair of accelerometers in the wings as input sensors, and it makes use of the autopilot normal accelerometers and the pitch augmentation rate sensors already on board the aircraft. System II (Figure 10) requires two additional pairs of dual accelerometers in each wing, and also requires the addition of dual-hydraulic servos to control the spoilers. A norm-rough weather switch is also required in the cockpit.

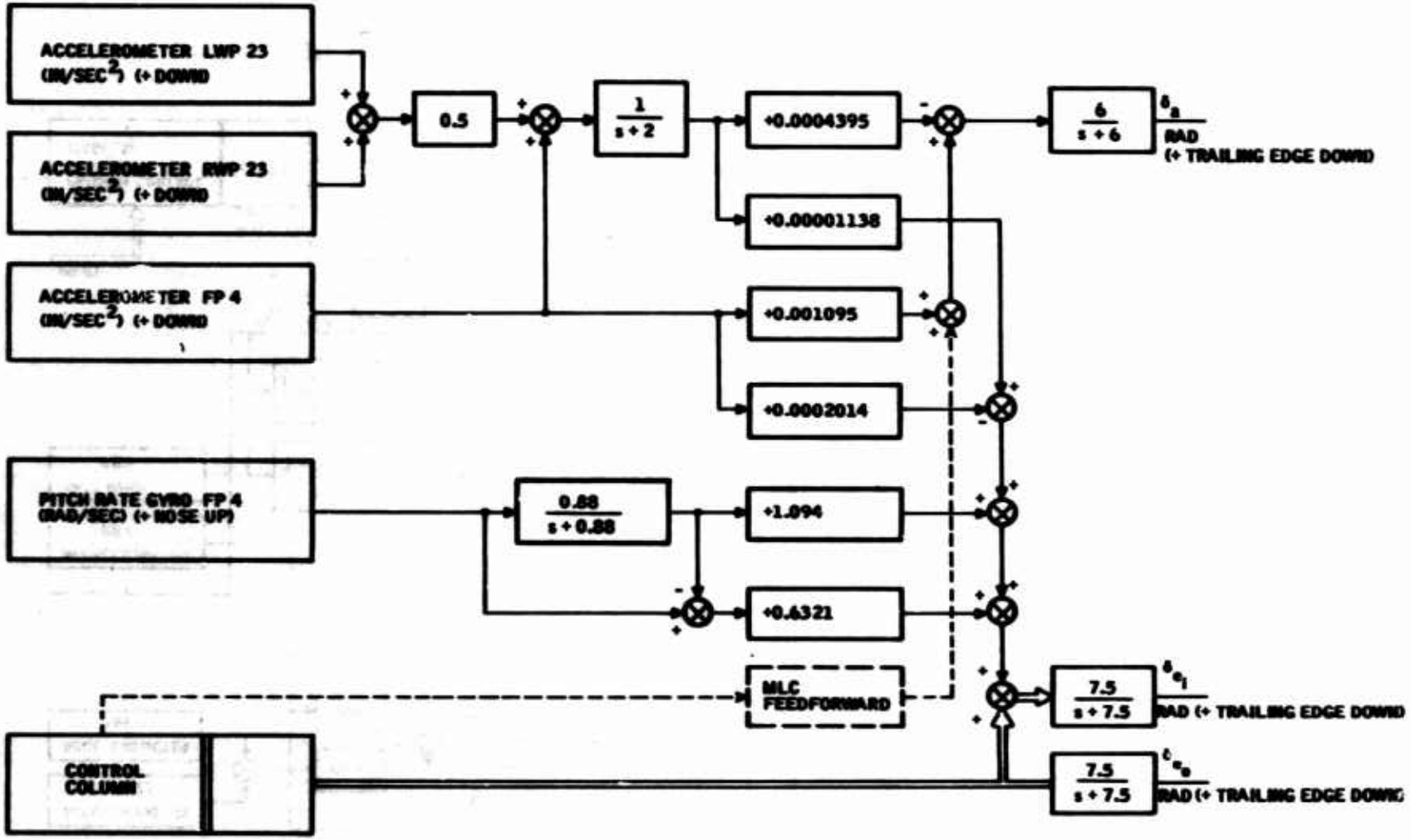

Figure 8. Simplified Control Block Diagram (Controller 14C)

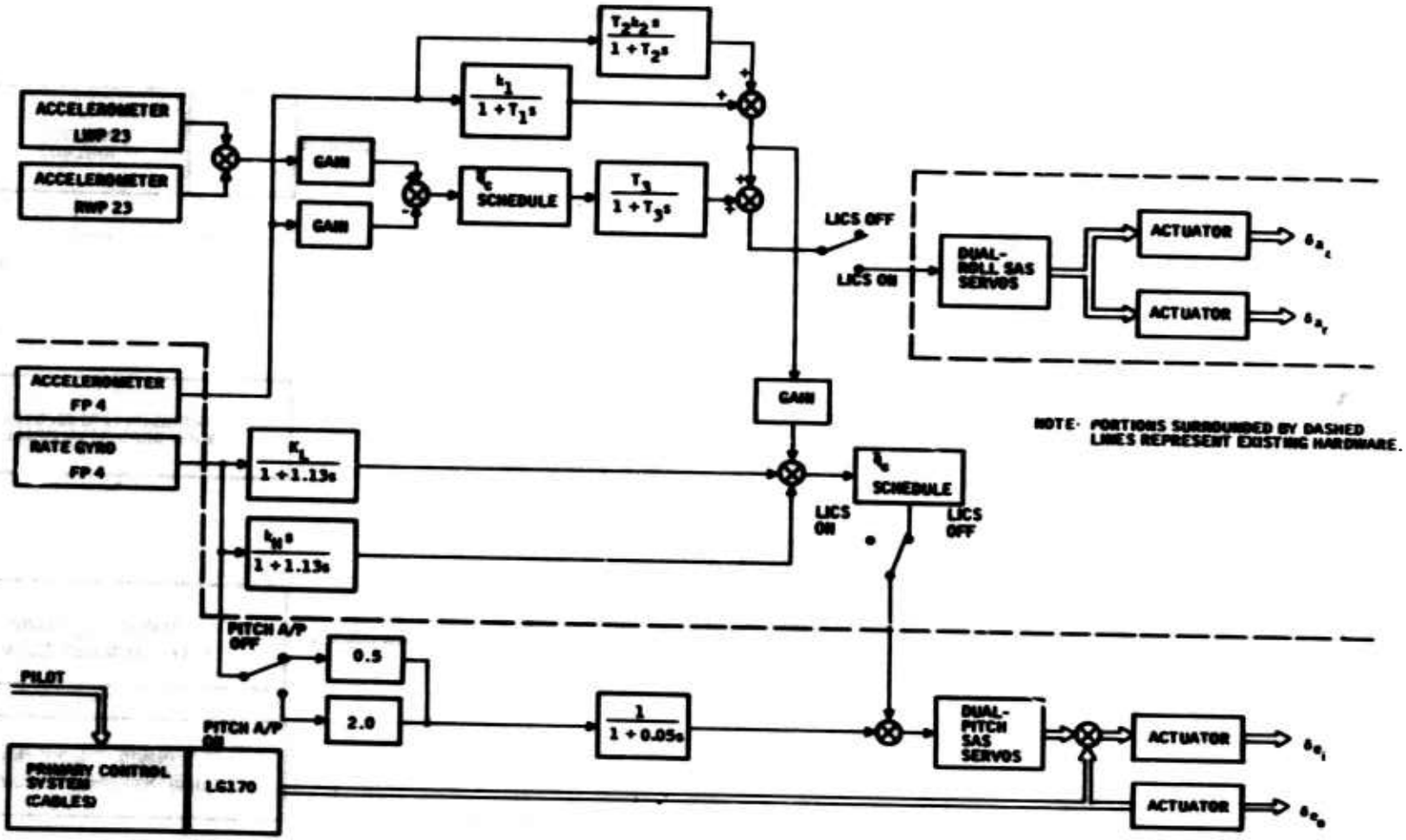

Figure 9. System I LICS (Without Spoilers) Block Diagram

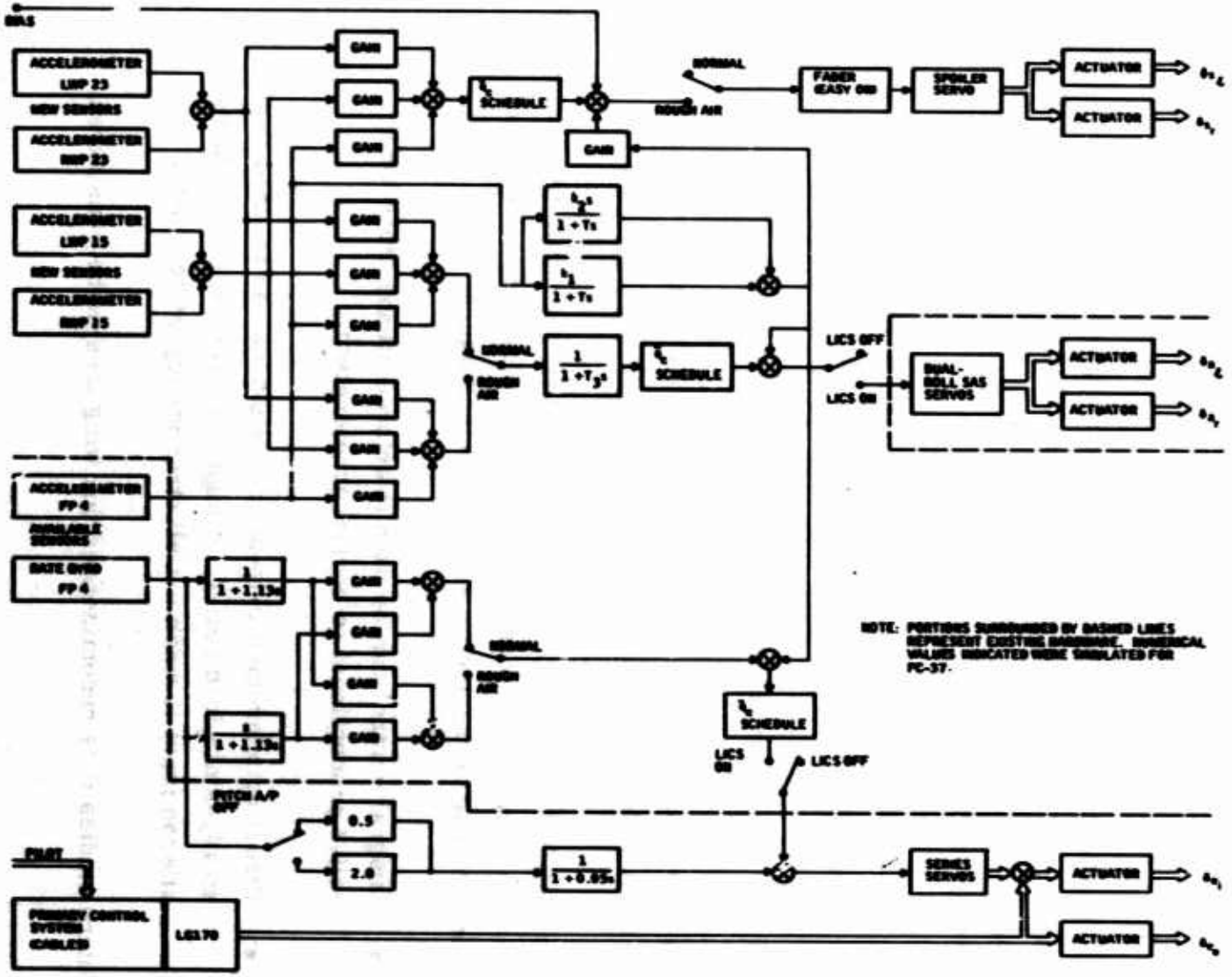

Figure 10. System II LICS (With Spoilers) Block Diagram

SECTION VI
CONCLUSIONS AND RECOMMENDATIONS

Results of the LICS study showed that rms wing root stress and stress rate can be reduced by factors of 50 percent and 31 percent, respectively, by using symmetric aileron and elevator control. However, two deficiencies become apparent:

- Handling qualities are degraded somewhat (this is noticeable when observing transients from step commands).
- No means for enforcing steady-state load relief are included.

At the time this report was being written, additional work had been done on the C-5A under contract from the Air Force.

Results from this study (Ref. 6) indicate that the handling qualities can be maintained with some loss in rms stress performance. The second deficiency can be corrected by at least two techniques:

- Integral control can be used to enforce steady-state load relief proportional to normal acceleration.
- Direct accelerometer-to-aileron feedback can be used to give steady-state load relief. A highpass network is used on the aileron input to wash out all other steady-state inputs.

In future studies it is recommended that wing torsion be considered.

APPENDIX
SYSTEM MATRICES FOR FLIGHT CONDITION 37

For the usual notation the model has the form

$$\dot{x} = Fx + G_1 u + G_2 \eta$$

$$r = Hx + Du$$

$$y = Mx$$

where

$$x^T = (w,\ \dot{\theta}/n_2,\ \dot{\eta}_1,\ \dot{\eta}_6,\ \dot{\eta}_3,\ \eta_1,\ \eta_6,\ \eta_3,\ \delta_a,\ \delta_e,\ p_1,\ p_2,\ p_3,\ p_4,\ p_5,\ p_6,\ w_g)$$

$$r^T = (s_1,\ s_2,\ \dot{s}_1,\ \dot{s}_2,\ \dot{\delta}_a,\ \dot{\delta}_e,\ \delta_a,\ \delta_e,\ \dot{\theta}/n_2)$$

and y is defined in Table VII.

The six matrices (F, G_1, G_2, H, D, and M) corresponding to flight condition 37 follow.

F MATRIX

```
ROW   1
  -.88108E+00  .40240E+01 -.96644E-01 -.56555E-01 -.00087E-01 -.10109E+01 -.52619E+01 -.58985E+01
  -.31709E+03 -.37302E+03  0.          0.          -.70224E+00 -.90114E+01 -.85945E+00  0.
   0.          -0.          0.
ROW   2
  -.46130E+00 -.12540E+01  .62222E-01  .11463E+01 -.53677E+00 -.38347E+00  .17116E+02 -.12928E+02
  -.69944E+03 -.31172E+04  0.          0.           .34791E+01 -.11270E+01 -.79140E+01  0.
   0.          -0.          0.
ROW   3
  -.15742E+01 -.14177E-01 -.18716E+01 -.12A30E+01 -.76911E+00 -.32155E+02 -.66123E+02 -.43979E+02
  -.30849E+04  .13649E+04  0.          0.           .95406E+00 -.22920E+02  .34748E+01  0.
   0.          -0.          0.
ROW   4
   .94887E+00  .42112E+00 -.37581E-01 -.12852E+01  .72948E-01  .58825E+00 -.37506E+03  .61900E+01
  -.28629E+03  .11659E+04  0.          0.           .29647E+00  .34633E+01  .29610E+01  0.
   0.          -0.          0.
ROW   5
   .72974E+00 -.33965E+00  .11730E+00  .91720E-01 -.13196E+01  .23756E+01  .16377E+02 -.21152E+03
  -.15308E+04 -.10142E+04  0.          0.          -.18097E+01  .14744E+02 -.41015E+01  0.
   0.          0.          0.
ROW   6
   0.          0.           .10000E+01  0.          0.          0.          0.          0.
   0.          0.          0.           0.          0.          0.          0.          0.
   0.          0.          0.
ROW   7
   0.          0.          0.           .10000E+01  0.          0.          0.          0.
   0.          0.          0.          0.           0.          0.          0.          0.
   0.          0.          0.
ROW   8
   0.          0.          0.          0.           .10000E+01  0.          0.          0.
   0.          0.          0.          0.          0.          0.          0.          0.
   0.          0.          0.
ROW   9
   0.          0.          0.          0.          0.          0.          0.          0.
  -.60000E+01  0.          0.          0.          0.          0.          0.          0.
   0.          0.          0.
ROW  10
   0.          0.          0.          0.          0.          0.          0.          0.
   0.         -.60000E+01  0.          0.          0.          0.          0.          0.
   0.          0.          0.
ROW  11
   0.           .53900E-03 -.67100E-04  .54300E-03 -.20000E-03  0.          0.          0.
   0.          0.         -.88100E+00  0.          0.          0.          0.          0.
   0.          0.          0.
ROW  12
   .10200E+01  .68997E+00  .19624E+01  .11328E+01  .14841E+01  .25860E+02  .27609E+03  .12553E+03
   .45760E+04  .72283E+03  0.          -.20000E+01 -.21679E+01  .12624E+02  .18098E+01  0.
   0.          0.          0.
ROW  13
   0.          0.          0.          0.          0.          0.          0.          0.
   0.          0.          0.          0.         -.37746E+02  0.          0.          0.
   0.          0.           .37746E+02
ROW  14
   0.          0.          0.          0.          0.          0.          0.          0.
   0.          0.          0.          0.          0.         -.10540E+02  0.          0.
   .10540E+02  0.          0.
ROW  15
   0.          0.          0.          0.          0.          0.          0.          0.
   0.          0.          0.          0.         -.42820E+01  0.          0.           .10000E+01
   0.          0.          0.
ROW  16
   0.          0.          0.          0.          0.          0.          0.          0.
   0.          0.          0.          0.           .13816E+03  0.         -.99211E+02 -.12566E+02
   0.          0.          0.
ROW  17
   0.          0.          0.          0.          0.          0.          0.          0.
   0.          0.          0.          0.          0.          0.          0.          0.
  -.19407E+02  0.           .19647E+02
ROW  18
   0.          0.          0.          0.          0.          0.          0.          0.
   0.          0.          0.          0.          0.          0.          0.          0.
   0.         -.69963E+00 -.10871E+00
ROW  19
   0.          0.          0.          0.          0.          0.          0.          0.
   0.          0.          0.          0.          0.          0.          0.          0.
   0.           .10000E+01  0.
```

G1 MATRIX

ROW	1	
	0.	0.
ROW	2	
	0.	0.
ROW	3	
	0.	0.
ROW	4	
	0.	0.
ROW	5	
	0.	0.
ROW	6	
	0.	0.
ROW	7	
	0.	0.
ROW	8	
	0.	0.
ROW	9	
	.60000E+01	0.
ROW	10	
	0.	.60000E+01
ROW	11	
	0.	0.
ROW	12	
	0.	0.
ROW	13	
	0.	0.
ROW	14	
	0.	0.
ROW	15	
	0.	0.
ROW	16	
	0.	0.
ROW	17	
	0.	0.
ROW	18	
	0.	0.
ROW	19	
	0.	0.

G2 MATRIX

ROW 1
0.
ROW 2
0.
ROW 3
0.
ROW 4
0.
ROW 5
0.
ROW 6
0.
ROW 7
0.
ROW 8
0.
ROW 9
0.
ROW 10
0.
ROW 11
0.
ROW 12
0.
ROW 13
0.
ROW 14
0.
ROW 15
0.
ROW 16
0.
ROW 17
0.
ROW 18
-.24279E+01
ROW 19
.51717E+01

H MATRIX

```
ROW   1
  -.441646E+01 -.10100E+01  .21979E+01  .21198E+00 -.92892E+00  .23771E+03 -.89482E+03 -.80479E+03
  -.59647E+03 -.28174E+04 0.           0.           .52507E+00 -.36571E+02 -.69392E+01 0.
  0.           0.           0.
ROW   2
  -.39122E+01 -.78588E+00  .11633E+01  .30215E+01  .28958E+01  .34865E+03  .17087E+04  .13507E+04
   .72448E+04 -.94651E+02 0.           0.           .28371E+01 -.51853E+02 -.34252E+00 0.
  0.           0.           0.
ROW   3
   .23222E-01 -.14163E+02  .23347E+03 -.89961E+03 -.80446E+03 -.74335E+02 -.24733E+03  .13144E+03
  -.21934E+04  .26500E+05 0.           0.           .26512E+02  .35849E+03  .24459E+02 -.69392E+01
  -.38548E+03 0.            .19819E+02
ROW   4
   .54955E+01 -.14090E+02  .34702E+03  .17025E+04  .13469E+04 -.24594E+02 -.11561E+04 -.61235E+03
  -.27417E+05  .47372E+04 0.           0.           -.10891E+03  .60820E+03  .10606E+02 -.34252E+00
  -.54655E+03 0.            .10789E+03
ROW   5
  0.           0.           0.           0.           0.           0.           0.           0.
  -.60000E+01 0.           0.           0.           0.           0.           0.           0.
  0.           0.           0.
ROW   6
  0.           0.           0.           0.           0.           0.           0.           0.
  0.           -.60000E+01 0.           0.           0.           0.           0.           0.
  0.           0.           0.
ROW   7
  0.           0.           0.           0.           0.           0.           0.           0.
   .10000E+01 0.           0.           0.           0.           0.           0.           0.
  0.           0.           0.
ROW   8
  0.           0.           0.           0.           0.           0.           0.           0.
  0.            .10000E+01 0.           0.           0.           0.           0.           0.
  0.           0.           0.
ROW   9
  0.           0.           0.           0.           0.           0.           0.           0.
  0.           0.           0.           0.           0.           0.           0.           0.
  0.           0.           0.
ROW  10
  0.           0.           0.           0.           0.           0.           0.           0.
  0.           0.           0.           0.           0.           0.           0.           0.
  0.           0.           0.
ROW  11
  0.           0.            .62222E-01  .11463E+01 -.53677E+00 -.38347E+00  .17116E+02 -.12920E+02
  -.60964E+03 -.31172E+04 0.           0.           0.           0.           0.           0.
  0.           0.           0.
ROW  12
   .10487E+01  .20650E+01  .62222E-01  .11463E+01 -.53677E+00 -.38347E+00  .17116E+02 -.12920E+02
  -.60964E+03 -.31172E+04 0.           0.          -0.          -0.           0.           0.
  0.           0.           0.
ROW  13
   .10000E+01 0.           0.           0.           0.           0.           0.           0.
  0.           0.           0.           0.           0.            .12000E+02 0.           0.
  0.           0.           0.
```

D MATRIX

```
ROW   1
  0.              0.
ROW   2
  0.              0.
ROW   3
  -.35788E+04 -.16880E+05
ROW   4
   .19596E+05 -.59191E+03
ROW   5
   .60000E+01 0.
ROW   6
  0.               .60000E+01
ROW   7
  0.              0.
ROW   8
  0.              0.
ROW   9
   .10000E+01 0.
ROW  10
  0.               .10000E+01
ROW  11
  0.              0.
ROW  12
  0.              0.
ROW  13
  0.              0.
```

M MATRIX

```
ROW   1
  0.          0.          0.          0.          .10000E+01  0.          0.          0.
  0.          0.          0.          0.          0.          0.          0.          0.
  0.          0.          0.
ROW   2
 -.52361E+00  .28051E+00 -.43035E-02 -.33407E+00 -.49263E-01  .11498E+01  .41867E+02 -.39266E+02
 -.62836E+02  .54414E+03  .14434E-03  0.          -.27225E+01 -.49650E+01  .14160E+01  0.
  0.          0.          0.
ROW   3
  .10208E+01  .68557E+00  .15624E+01  .11324E+01  .14861E+01  .25860E+02  .27609E+03  .12553E+03
  .45740E+04  .72243E+03  0.          0.          -.21679E+01  .12624E+02  .1809WE+01  0.
  0.          0.          0.
ROW   4
  0.          0.          .10000E+01  0.          0.          0.          0.          0.
  0.          0.          0.          0.          0.          0.          0.          0.
  0.          0.          0.
ROW   5
  .11323E+01  .60211E+00  .41254E+00 -.44491E+00 -.25548E+00  .84145E+01 -.95265E+02 -.97822E+02
  .25706E+03  .81874E+03  0.          0.          -.29044E+01  .14434E+02  .20707E+01  0.
  0.          0.          0.
ROW   6
  .64879E+00  .47631E+00  .11950E+00 -.51030E+00 -.26818E+00  .29721E+01 -.17802E+02 -.82524E+02
 -.13528E+03  .78301E+03  0.          0.          -.24954E+01  .83080E+01  .19849E+01  0.
  0.          0.          0.
ROW   7
  0.          0.          0.          .10000E+01  0.          0.          0.          0.
  0.          0.          0.          0.          0.          0.          0.          0.
  0.          0.          0.
ROW   8
  0.          0.          0.          0.          0.          0.          0.          0.
  0.          0.          .10000E+01  0.          0.          0.          0.          0.
  0.          0.          0.
ROW   9
  0.          0.          0.          0.          0.          0.          0.          0.
  .10000E+01  0.          0.          0.          0.          0.          0.          0.
  0.          0.          0.
ROW  10
  0.          0.          0.          0.          0.          0.          0.          0.
  0.          .10000E+01  0.          0.          0.          0.          0.          0.
  0.          0.          0.
ROW  11
  0.          0.          0.          0.          0.          0.          0.          0.
  0.          0.          0.          0.          0.          0.          0.          0.
  0.          0.          .10000E+01
ROW  12
  0.          0.          0.          0.          0.          0.          0.          0.
  0.          0.          0.          0.          .10000E+01  0.          0.          0.
  0.          0.          0.
ROW  13
  0.          0.          0.          0.          0.          0.          0.          0.
  0.          0.          0.          0.          0.          .10000E+01  0.          0.
  0.          0.          0.
ROW  14
  0.          0.          0.          0.          0.          0.          0.          0.
  0.          0.          0.          0.          0.          0.          .10000E+01  0.
  0.          0.          0.
ROW  15
  0.          0.          0.          0.          0.          0.          0.          0.
  0.          0.          0.          0.          0.          0.          0.          .10000E+01
  0.          0.          0.
ROW  16
  0.          0.          0.          0.          0.          0.          0.          0.
  0.          0.          0.          0.          0.          0.          0.          0.
  .10000E+01  0.          0.
ROW  17
  0.          0.          0.          0.          0.          0.          0.          0.
  0.          0.          0.          0.          0.          0.          0.          0.
  0.          .10000E+01  0.
ROW  18
  0.          .40640E-03 -.76234E-04  .61692E-03 -.78438E-03  0.          0.          0.
  0.          0.          -.10000E+01 0.          0.          0.          0.          0.
  0.          0.          0.
ROW  19
  0.          0.          0.          0.          0.          0.          0.          0.
  0.          0.          0.          .10000E+01  0.          0.          0.          0.
  0.          0.          0.
```

REFERENCES

1. VanDierendonck, A.J., "Practical Optimal Flight Control for Aircraft with Large Flight Envelopes," AIAA Paper No. 73-159, AIAA 11th Aerospace Sciences Meeting, January 1973.

2. VanDierendonck, A.J., "Practical Quadratic Optimal Control for Systems with Large Parameter Variations," Conference Record, Sixth Asilomar Conference on Circuits and Systems, pp. 391-396, November 1972.

3. Stone, C.R., Ward, M.D., Harvey, C.A., Ebsen, M.E., McBridle, E.E., and Hollenbeck, W.W., "Studies on the Compatibility of Relaxed Static Stability and Maneuver Load Control to C-5A-Type Aircraft," Volumes I and II, Technical Report AFFDL-TR-72-38, Wright-Patterson Air Force Base, Ohio, June 1972.

4. Edinger, L. and Lahn, T., "C-5A Data Base for Load Alleviation and Mode Stabilization Program," Report 20564-DB1, Honeywell Inc., Government and Aeronautical Products Division, Minneapolis, Minnesota, 1 April 1968.

5. Anonymous, "Aircraft Load Alleviation and Mode Stabilization (LAMS): C-5A System Analysis and Synthesis," Technical Report AFFDL-TR-68-162, Wright-Patterson Air Force Base, Ohio, November 1969.

6. Barrett, M.F. and McLane, R.C., "Procedure and Results for ALDCS Task III, Subtask IB (Part 1) (Old LICS Continuation at FC-37)," Honeywell Inc. Memorandum MR-12223, 4 September 1973.